

Energy & Environmental Science

Accepted Manuscript



This is an *Accepted Manuscript*, which has been through the Royal Society of Chemistry peer review process and has been accepted for publication.

Accepted Manuscripts are published online shortly after acceptance, before technical editing, formatting and proof reading. Using this free service, authors can make their results available to the community, in citable form, before we publish the edited article. We will replace this *Accepted Manuscript* with the edited and formatted *Advance Article* as soon as it is available.

You can find more information about *Accepted Manuscripts* in the [Information for Authors](#).

Please note that technical editing may introduce minor changes to the text and/or graphics, which may alter content. The journal's standard [Terms & Conditions](#) and the [Ethical guidelines](#) still apply. In no event shall the Royal Society of Chemistry be held responsible for any errors or omissions in this *Accepted Manuscript* or any consequences arising from the use of any information it contains.

Spinel Compounds as Multivalent Battery Cathodes: A Systematic Evaluation Based on *ab initio* Calculations

Miao Liu^{1**}, Ziqin Rong^{2**}, Rahul Malik², Pieremanuele Canepa², Anubhav Jain¹, Gerbrand Ceder², and Kristin Persson^{1*}

¹Environmental Energy Technologies Division, Lawrence Berkeley National Laboratory, CA 94720, USA

²The Department of Materials Science and Engineering, Massachusetts Institute of Technology, Cambridge MA 02139, USA

*Corresponding author email: kapersson@lbl.gov

**M. Liu and Z. Rong contributed equally to this work.

Abstract

Batteries that shuttle multi-valent ions such as Mg^{2+} and Ca^{2+} ions are promising candidates for achieving higher energy density than available with current Li-ion technology. Finding electrode materials that reversibly store and release these multi-valent cations is considered a major challenge for enabling such multi-valent battery technology. In this paper, we use recent advances in high-throughput first-principles calculations to systematically evaluate the performance of compounds with the spinel structure as multivalent intercalation cathode materials, spanning a matrix of five different intercalating ions and seven transition metal redox active cation. We estimate the insertion voltage, capacity, thermodynamic stability of charged and discharged states, as well as the intercalating ion mobility and use these properties to evaluate promising directions. Our calculations indicate that the Mn_2O_4 spinel phase based on Mg and Ca are feasible cathode materials. In general, we find that multivalent cathodes exhibit lower voltages compared to Li cathodes;

the voltages of Ca spinels are $\sim 0.2\text{V}$ higher than those of Mg compounds (versus their corresponding metals), and the voltages of Mg compounds are $\sim 1.4\text{ V}$ higher than Zn compounds; consequently, Ca and Mg spinels exhibit the highest energy densities amongst all the multivalent cation species. The activation barrier for the Al^{3+} ion migration in the Mn_2O_4 spinel is very high ($\sim 1400\text{ meV}$ for Al^{3+} in the dilute limit); thus, the use of an Al based Mn spinel intercalation cathode is unlikely. Amongst the choice of transition metals, Mn-based spinel structures rank highest when balancing all the considered properties.

Broader Context

The high price and limited volumetric capacity of the lithium ion battery (LIB) challenges its application in electric vehicles and portable electronics. Multivalent batteries, such as those utilizing Mg^{2+} or Ca^{2+} as the working ions, are promising candidates for beyond LIB technology due to the increase in volumetric capacity and reduced cost. In the present work, we use first-principles calculations to systematically evaluate the theoretical performance of the spinel structure host with the general formula AB_2O_4 across a matrix of chemical compositions spanning $\text{A}=\{\text{Al}, \text{Y}, \text{Mg}, \text{Ca}, \text{Zn}\}$ and $\text{B}=\{\text{Ti}, \text{V}, \text{Cr}, \text{Mn}, \text{Fe}, \text{Co}, \text{Ni}\}$ for multivalent battery applications. The evaluation incorporates screening on voltage, capacity, thermodynamic structural and thermal stability as well as ion mobility and discusses the results in the context of available host structure sites, preference of the intercalating cation, and the oxidation state of the redox-active cation. Overall, the Mn_2O_4 spinel phases paired with Mg^{2+} or Ca^{2+} emerge as the most promising multivalent cathode materials. As the first comprehensive screening of multivalent intercalation compounds across size, valence, and redox-states of the involved cations, our work is intended to

provide guidance for future theoretical as well as experimental multivalent cathode development and design.

Introduction

To support the rapidly growing energy storage demands of future technologies such as electric vehicles, improved battery technologies are needed. Lithium (Li) ion batteries with good energy density, rechargeability and cycle life¹ have been used to advance portable consumer electronics and recently, electric vehicles. However, further advancement of Li ion technology faces limits on the energy density of electrode materials^{2,3}, safety, and high cost. A multivalent battery technology, where an intercalation cathode host is paired with a metal anode, has the potential to store energy at significantly lower cost and volume.⁴⁻⁶ For example, Mg metal has much higher volumetric capacity (3833 mAh/cc) than graphite (~ 800 mAh/cc)^{7,8} or even lithium metal (2046 mAh/cc). Furthermore, as many known intercalation hosts are limited by the available cation insertion sites rather than by redox capability, one can expect improvements using multivalent intercalation on the cathode side. For instance, Mg²⁺ carries two charges per ion while maintaining an ionic radius as small as that of a Li⁺ ion, hence the charge storage capability is doubled at the same cation volumetric concentration. In addition, the natural abundance of multivalent elements, such as Mg and Ca, is significantly higher than that of Li (the atomic abundance of Mg is ~10⁴ times larger than Li in earth crust), which may decrease the cost of materials and guarantee supply even for multi-fold increases in the size of the energy storage market.

To date, there have been limited examples demonstrating the feasibility of

rechargeable multivalent batteries, and among them, most of the focus has been on Mg technology. In the seminal work of Aurbach et al, it was demonstrated that Mg^{2+} can intercalate into the Chevrel phase Mo_6S_8 at a potential of ~ 1.0 - 1.3 V and a maximum charge capacity of 135 mAh/g for several hundreds of cycles^{6,9}. Other materials have shown initial promise for multi-valent intercalation, such as layered V_2O_5 where Mg^{2+} is inserted into the V_2O_5 inner layer spacing^{10,11}. Ca^{2+} has also been shown to intercalate into V_2O_5 , supplying a voltage of ~ 3.0 V and an initial capacity of ~ 450 mAh/g.¹² Other materials claimed to accommodate Mg^{2+} insertion include MoO_3 ¹³⁻¹⁵, TiS_2 in both the cubic phase and layered phases¹⁶, NbS_3 ¹⁷, graphitic fluoride¹⁸, and CoSiO_4 ¹⁹. However, due to limited Mg mobility in the host and possibly concurrent water and/or proton insertion, the cycling stability of these materials has so far been insufficient, resulting in rapid decomposition of the host material^{20,21}.

From the limited experimental studies performed to date, the feasibility of a battery technology based on multivalent intercalation is not yet clear. As the cathode will be a critical component of such a technology, it is important to assess the feasibility of multi-valent insertion cathodes. In this work, we present a systematic computational study of multivalent intercalation within a fixed spinel-based host structure, using a set of seven redox-active cations and spanning size and valence differences between a set of intercalating {Ca, Zn, Mg, Al and Y} cations to establish design trends and guidelines for future experimental work.

The spinel (prototype MgAl_2O_4 , space group $\text{Fd-}3\text{m}$) structure provides an excellent candidate for this study, encompassing a family of materials with the general formula AB_2O_4 . The A and B ions are tetrahedrally and octahedrally coordinated by oxygen, respectively (Figure 1). The B octahedrons form a network with percolating empty sites interconnecting in three directions. Spinel LiMn_2O_4 was first prepared by M. M. Thackeray et al²² and exhibits excellent performance as a cathode for Li intercalation with a voltage of 3-4 V versus Li metal²³. The properties of the spinel structure are tunable, for example it has been observed that partially replacing Mn with Ni increases the voltage to 4.7 V,^{24,25} and mixing Mn with Co and/or Cr increases the voltage even higher to ~ 5 V.²⁵⁻²⁷

Experiment shows that spinel LiMn_2O_4 can be electrochemically converted to MgMn_2O_4 in aqueous $\text{Mg}(\text{NO}_3)_2$ electrolyte, and exhibits Mg^{2+} reversible intercalation/deintercalation²⁸. Spinel ZnMnO_2 has also demonstrated Zn^{2+} insertion/deinsertion, providing a capacity of 210 mAh/g for 50 cycles²⁹. Recently, it was shown that Mg^{2+} can intercalate/deintercalate into spinel-type Mn_2O_4 with a retained capacity of 155.6 mAh/g after 300 cycles in 1 mol dm^{-3} MgCl_2 aqueous electrolyte³⁰, suggesting that further development could lead to a viable cathode with good energy density. Against this background it is intriguing to broadly consider a multivalent spinel cathode with possible intercalating cations $A = \{\text{Mg}, \text{Ca}, \text{Zn}, \text{Al}, \text{Y}\}$ that could theoretically produce a higher capacity than its Li counterpart due to the greater charge carried by each ion. Hence, in this paper, our aim is to evaluate the cathode performance of spinel phases for multi-valent intercalation; we computationally evaluate the feasibility of a matrix of spinel compounds with

different redox ion species and intercalating cation species. The redox ion was selected from the set {Ti, V, Cr, Mn, Fe, Co, Ni}, and the intercalating cation was selected from the set {Mg, Ca, Zn, Al, Y}. By substituting the cations in the A and B sites, respectively, we created 35 charged/discharged topotactic pairs and performed first-principles density functional theory (DFT) calculations for each of these pairs. We evaluate cathode performance through such quantities as the capacity, average voltage, energy density, and intercalating cation mobility. We also evaluate the thermodynamic structural and thermal stability. The detailed methodology can be found in previous literature³¹.

Methods

We use the Vienna *ab initio* software package (VASP)³² to perform the density functional theory calculations, with the projector augmented-wave method³³ to describe the ion-electron interactions and the generalized gradient approximation (GGA)³⁴ within the Perdew-Burke-Ernzerhof (PBE) framework³⁵ as the exchange-correlation functional. The calculation parameters are the same as those adopted by the Materials Project³⁶ and as implemented in the pymatgen software package³⁷, which have been previously tested to be appropriate to study Li-intercalation cathode materials³¹. In the calculations, the U - J parameters to correct for non-cancellation of the self-interaction error in the d orbitals of the redox active species are set to $U_V = 3.25$ eV, $U_{Cr} = 3.7$ eV, $U_{Mn} = 3.9$ eV, $U_{Fe} = 5.3$ eV, $U_{Co} = 3.32$ eV, and $U_{Ni} = 6.45$ eV.³⁸ The primitive spinel unit cell as illustrated in Figure 1 is used for voltage and stability calculations. Brillouin zone sampling is performed on a $5 \times 5 \times$

5 grid in k -space. Throughout this work, the cell shape, volume and atomic positions are relaxed, unless otherwise stated. All magnetic ions are initialized ferromagnetically.

All calculations in this paper assume that the transition metal host framework 'B₂O₄' remains structurally invariant during the operation of the battery (i.e., during intercalation and de-intercalation of 'A' cations). Additionally, we assume that the host can be synthesized with little/no disorder and remains that way during the operation of the cell. We acknowledge that spinels are well known to show varying degrees of cation disorder that may impact important material properties relevant for battery operation such as the activation energies and voltages reported herein. However, in the interest of providing a preliminary view of what is possible in multivalent systems, we have simplified our calculations and analysis.

The voltages of the compounds can be obtained from the difference in the total energy between the charged and discharged phases following Aydinol *et al.*^{39,40}. The average voltage can be calculated as $\bar{V} = \Delta E / nz$, where $\Delta E = (E_{charge} + E_{MV} - E_{discharge})$ denotes the total energy change in the reaction, E_{charge} and $E_{discharge}$ are the energy of the charged and discharged compounds respectively; E_{MV} is the energy of multivalent intercalating species in metal form; n is number of intercalating atoms participated in the reaction; and the z represents the oxidation states of the intercalant. We adopt the units of eV and e for ΔE and nz , respectively, so that no

normalization factor (i.e., Faraday's constant) needs to be introduced into the equation. We estimate the thermodynamic stability of the phases by the energy above the convex hull of stable phases, which is the energy released by decomposing the compound to the most stable combination of compounds at the same overall composition^{41,42}. The energy above the hull is always a non-negative number with the unit of eV/atom. The detailed procedure for the computation of the energy above the hull can be found in previous literature^{41,42}. As explained later in this paper, the thermal stability was determined by evaluating the critical chemical potential at which O₂ gas becomes favorable according to the methodology presented in Ong *et al.*⁴³. Since the entropy of a reaction is dominated by the gas entropy and the entropy of the solid phase at room temperature³⁸, for the any reactions containing molecular O₂, we use the corrected O₂ chemical potential to include the well-known O₂ DFT calculation error³⁸ as well as the $P\Delta V$ contribution to the oxygen enthalpy⁴³ by comparing with the experimental thermodynamic data⁴⁴ for O₂ at 0.1 MPa at 298K throughout the paper. For the thermal stability calculation, the temperature effect has been taken into account by adjusting the entropy term ($-T\Delta S$) of the O₂ chemical potential at given temperature⁴⁵. A more detailed description can be found in the online supplementary information.

The calculations were automatically executed and analyzed using the *FireWorks* software package⁴⁶. In this work, hundreds of DFT calculations are performed across 70 compounds to generate the thermodynamic stability and thermal stability data^{41,43}.

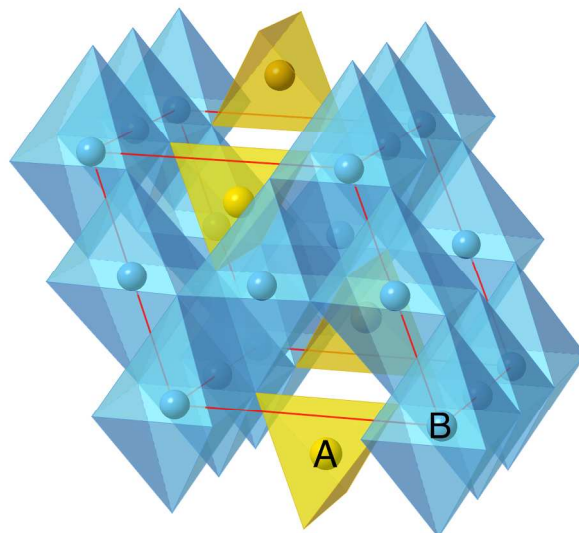


Fig. 1. The spinel crystal structure where the 'A' atoms occupy the tetrahedral sites, and the 'B' atoms occupy the octahedral site. Throughout this paper, the 'A' atoms are multivalent intercalating ions selected from the set $\{\text{Mg}^{2+}, \text{Ca}^{2+}, \text{Zn}^{2+}, \text{Y}^{3+}, \text{Al}^{3+}\}$, and the 'B' atoms are transition redox-active ions, selected from the set $\{\text{Ti}, \text{V}, \text{Cr}, \text{Mn}, \text{Fe}, \text{Co}, \text{Ni}\}$.

Activation barriers were calculated with the nudged elastic band (NEB) method⁴⁷ using the GGA-PBE functional^{34,35}. A U term was not included in these calculations as NEB is difficult to converge with GGA+ U due to pronounced metastability of electronic states along the ion migration path. Furthermore, while GGA+ U clearly improves the accuracy of redox reactions³¹, there is no conclusive evidence that GGA+ U performs better in predicting cation migration⁴⁸⁻⁵². The minimum energy paths (MEP) in the NEB procedure were initialized by linear interpolation of 8 images between the two fully relaxed end-point geometries, and each image is converged to $< 1 \times 10^{-4}$ eV/super cell. The MEPs were obtained in both the high vacancy limit and dilute vacancy limit, i.e. one mobile species per unit cell or one vacancy per unit cell. To ensure that fictitious interactions between the diffusing species are removed, a $2 \times 2 \times 2$ supercell of the primitive cell was used, for which

the inter-image distance is never less than 8 Å.

Results and Discussion

The average intercalation voltage was calculated from the reaction energy $B_2O_4 + A > AB_2O_4$ for the matrix of intercalating $A = \{Mg, Ca, Zn, Y, Al\}$ ions and redox active transition metals $B = \{Ti, V, Cr, Mn, Fe, Co, Ni\}$ metal cations. Figure 2 shows the resulting voltage vs. the gravimetric capacity. The color and shape of a data point indicate the intercalating ion, and the redox-active transition metal is given next to each data point. Voltages are referenced to the bulk metal of the intercalating ion, e.g., Mg metal for $MgMn_2O_4$ and Zn metal for $ZnMn_2O_4$.

As expected from the electrochemical series, and evidenced in Figure 2, multivalent compounds have lower voltages than Li cathodes. The Li ion spinel usually exhibits a voltage between 4 and 5 V,^{22,26,53} whereas we find that for multivalent spinel cathodes, the voltage is always less than 4 V versus the corresponding metal. Most Mg and Ca intercalation voltages vary between 2 and 4 V, which is lower than the values for Li (e.g., calculated voltage of $LiMn_2O_4$ is ~0.7 V higher than $CaMn_2O_4$)^{22,54}; however, considering the additional charge carried by multivalent cations, a multivalent spinel cathode can still exhibit a significantly higher energy density than the corresponding Li version. For example, the gravimetric capacity of $LiMn_2O_4$ is 143 mAh/g,^{22,36} whereas the gravimetric capacity of $MgMn_2O_4$ is almost double ~270 mAh/g, which more than makes up for the slightly lower voltage. Hence, of the considered intercalating ions, Al, Y, Ca and Mg are all viable candidates from the perspective of energy density. However, the voltage of the Zn spinel compounds

ranges between 1.3- 2.5 V, which even in the best case scenario amounts to approximately 600 Wh/kg, about equal to specific energy of LiFePO_4 ^{36,43}.

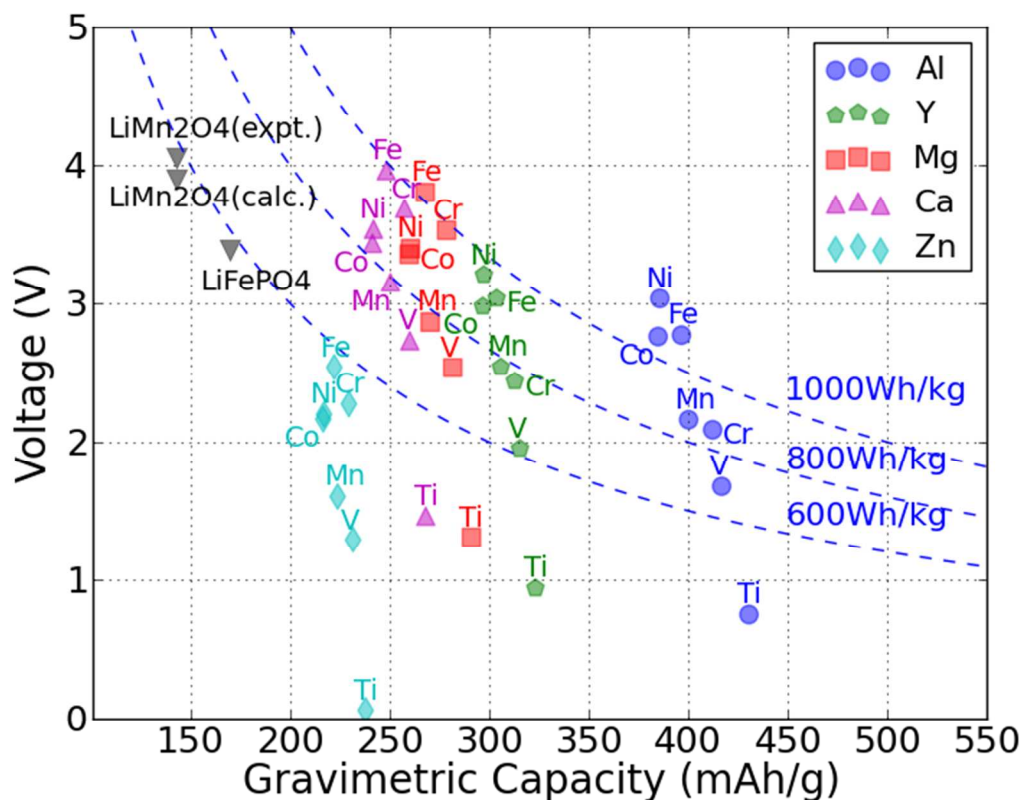


Fig. 2. The computed average voltage vs. gravimetric capacity for intercalation of A = Zn, Ca, Mg, Y and Al in various M_2O_4 spinels up to composition AM_2O_4 . The redox-active metal is marked next to each point. Dashed curves show the specific energy of 600Wh/kg, 800Wh/kg and 1000Wh/kg, respectively. The spinel LiMn_2O_4 and olivine LiFePO_4 data points are also marked on the plot for comparison^{22,36,43}.

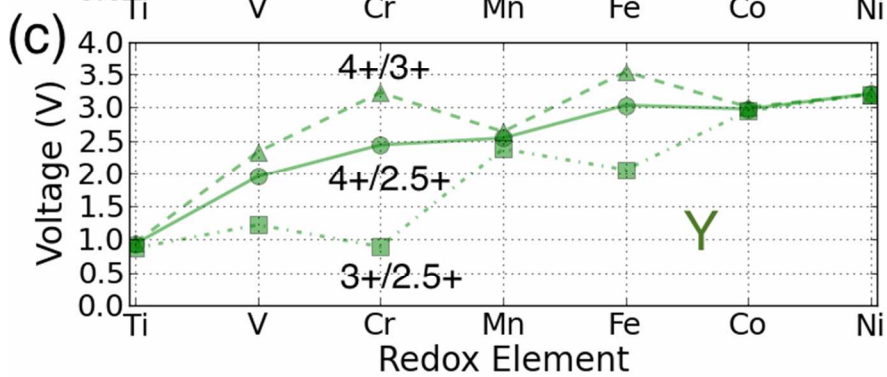
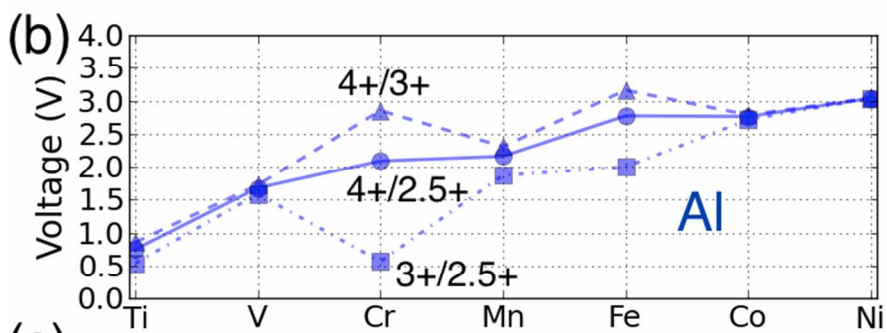
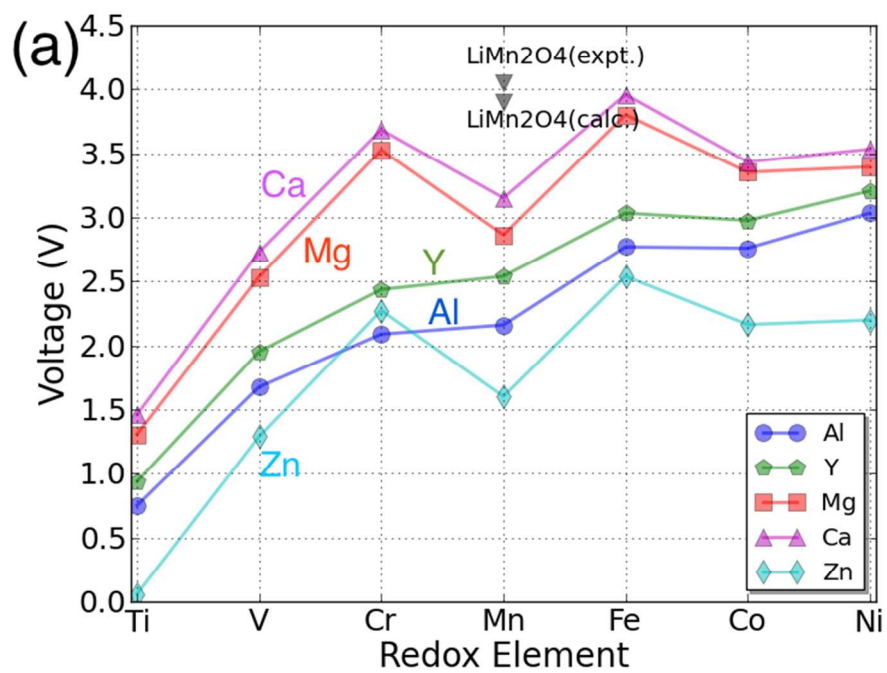


Fig. 3. (a) The calculated voltage of each spinel phase for the reaction $B_2O_4 + A \rightarrow AB_2O_4$ as a function of the redox-active transition metal and intercalating cation. The different colors denote different intercalating species as specified by the legend. The black triangle point indicates the data corresponding to the spinel $LiMn_2O_4$ ^{22,36}; (b) and (c): For Y and Al the voltage for separate 3+/2.5+ and 4+/3+ redox reactions is compared to the overall voltage for the 4+/2.5+ redox change corresponding to the full intercalation range, as in (a).

The voltage for each multi-valent intercalant is plotted as a function of the active redox metal in Figure 3(a): The bi-valent ions Ca, Mg, and Zn follow a common trend as the redox couple is varied, different from the voltage trend of the tri-valent intercalants Al and Y. The difference originates largely from the different valence state of the transition metal in the discharged state. Insertion of the bi-valent cations induces a change in redox state from 4+ to 3+, whereas the tri-valent cation corresponds to a redox change from 4+ to 2.5+ for insertion to AB_2O_4 .

In general, the Ca spinel has the highest voltage, followed by the Mg spinel compounds, Y compounds, Al compounds, and Zn compounds, in that order. For all the redox active cations {B = Ti, V, Cr, Mn and Ni} the voltage of the Mg compounds is lower than that of the Ca compounds by ~0.2 V, and the voltages of Mg compounds are ~1.4 V higher than Zn compounds. The three bi-valent intercalants show the same trend of voltage verses redox active metal: Ti_2O_4 always has the lowest voltage among the transition metals considered. V_2O_4 is the second lowest one but ~1.2V higher than Ti_2O_4 . Mn_2O_4 is ~0.3 V higher than V_2O_4 , Co_2O_4 is ~0.6 V

higher than Mn_2O_4 , and Ni_2O_4 is slightly higher than Co_2O_4 by ~ 0.1 V. The Cr_2O_4 and Fe_2O_4 spinels have the highest voltage, respectively ~ 0.6 V and ~ 0.9 V higher than Mn_2O_4 . Bhattacharya *et al.* found a similar trend for the Li insertion voltage in these spinels⁵⁴. We find that Li insertion⁵⁴ occurs on average at about ~ 0.7 V higher voltage than Ca insertion and ~ 0.9 V higher than Mg insertion. Comparing this with the aqueous electrochemical series ($E^0_{\text{Li}} = -3.04$, $E^0_{\text{Ca}} = -2.86$, $E^0_{\text{Mg}} = -2.37$, $E^0_{\text{Zn}} = -0.76$) we find that the voltages are ordered according to the electrochemical series of the intercalating metal ion. However, while the voltage shift between Li and Mg is close to what is expected, the voltage reduction in moving from Li to Ca in the solid state is considerably larger than expected from the electrochemical series. This is likely due to the fact that the intercalant enters a tetrahedral site in the spinel, which for Ca is not nearly as favorable as for Mg and Li, and thus reduces the Ca intercalation voltage from what one would expect from the electrochemical series. Experimentally, Li has indeed been found to exhibit a higher voltage than Mg. In the Chevrel phase Mo_6S_8 , the voltage difference between Li and Mg insertion is ~ 1.0 - 1.2 V^{9,55,56}. For V_2O_5 , the Li voltage is usually ~ 0.2 V higher than that of Mg⁵⁷⁻⁵⁹. Because the data in Figure 3(a) for trivalent cations averages the voltage over both the $3+/2.5+$ and $4+/3+$ redox couples, the intermediate $3+$ states of the transition metals were calculated for the trivalent intercalants to investigate the impact of different redox states. Figure 3(b) and (c) show the calculated voltage of the different redox pairs for the Al and Y spinel compounds, respectively. As expected, the $3+/2.5+$ redox pairs exhibit a lower voltage compared to the $4+/3+$ reactions, in good agreement with existing literature². In particular, when restricting focus to the

4+/3+ redox reaction, the Al and Y spinel compounds follow largely the same trend with Ca, Mg and Zn as shown in Figure 3(a).

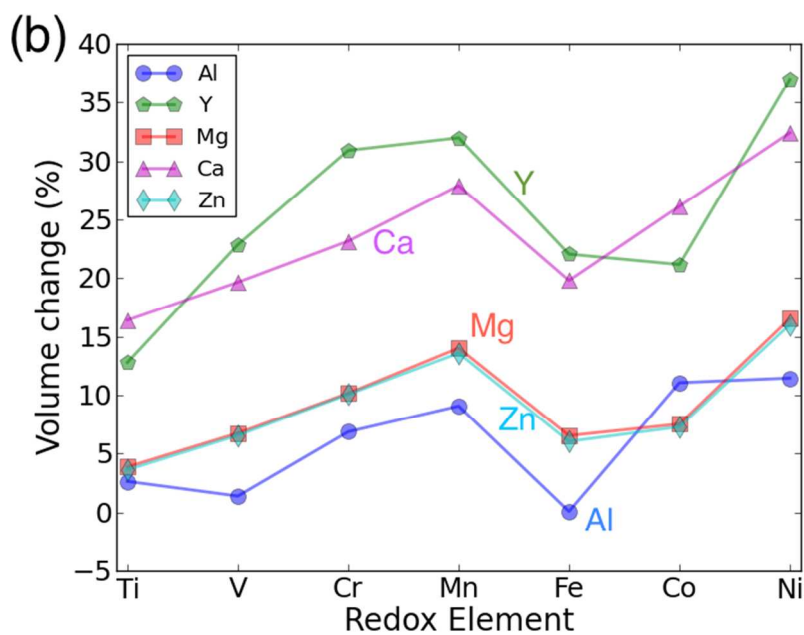
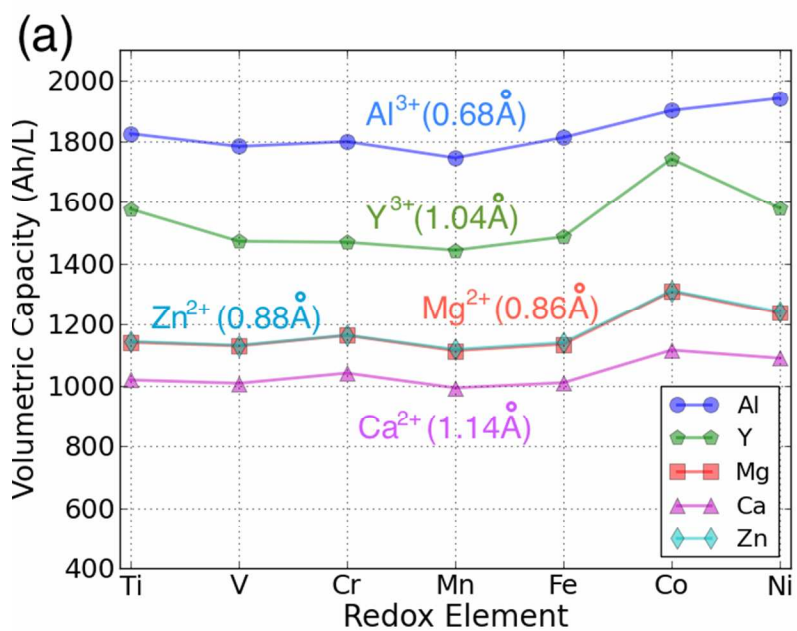


Fig. 4 The calculated (a) volumetric multivalent capacity and (b) volume change of the spinel structure as a function of the redox-active cation, assuming intercalation to composition AB_2O_4 .

The capacity density of cathode materials is important as it strongly influences the overall energy density of a cell. Figure 4 (a) shows the volumetric capacity of each AB_2O_4 spinel as a function of the redox-active species and intercalating cation. The volumetric capacity of all the cathodes is higher than that of a Li spinel cathode at the same cation concentration due to the extra charge carried by each of the multi-valent intercalants. Not surprisingly, Al^{3+} leads to the highest capacity density, while Ca^{2+} has the lowest. For a fixed valence of the intercalant, the volumetric capacity follows the ionic size of the intercalating cation. Hence, the volumetric capacities of Al^{3+} compounds are higher than Y^{3+} compounds by approximately 300 Ah/L. For bi-valent cations, the capacities of Mg and Zn compounds are almost the same consistent with the similar ionic size of Mg^{2+} or Zn^{2+} .

Figure 4(b) presents the volume expansion associated with the intercalation of each multi-valent ion as function of the redox metal. Volume change is an important parameter as it needs to be accommodated at the particle, electrode and cell level. At the particle level, large volume changes can lead to particle fracture and loss of contact. The total volume change associated with intercalation is the combined result of the intercalant insertion and the transition metal reduction, and can be very small for some Li-insertion systems^{60,61}. The contribution from the

intercalating ion will depend on its size and charge. For example, Y^{3+} leads to larger volume increase than Al^{3+} as the ion is much larger. The effect of charge cannot as easily be extracted from Fig 4b as the +3 cations also cause a larger reduction of the transition metal than the 2+ cations. Reduction of the transition metals generally leads to an increase in volume, although the magnitude of the change depends on the nature of the metal- d orbital that is being filled. Filling of t_{2g} orbitals, which are to first order non-bonding⁴⁰, tends to cause only a small increase in volume, while the anti-bonding e_g orbitals lead to a larger volume change⁶⁰. This explains why in general the early transition metals, such as Ti and V exhibit lower volume changes. They have several unoccupied t_{2g} orbitals, which are available for reduction. On the other hand, Mn and Ni-based spinels show the largest volume changes as their reduction occurs by filling one or more e_g orbitals. For both Mn^{3+} and Ni^{3+} this volume increase is compounded by the fact that these ions are Jahn-Teller active which, in its anharmonic form, leads to additional volume increase⁶². The combined small size and high charge of Al^{3+} lead to almost zero volume change for several spinels.

For Mg, Zn and Al insertion, the magnitude of the volume change normalized by the capacity is very similar to the volume changes observed for Li insertion compounds, and hence is not likely to lead to any practical design problems. For Ca and Y the volume change is larger - up to 30% increase in some cases.

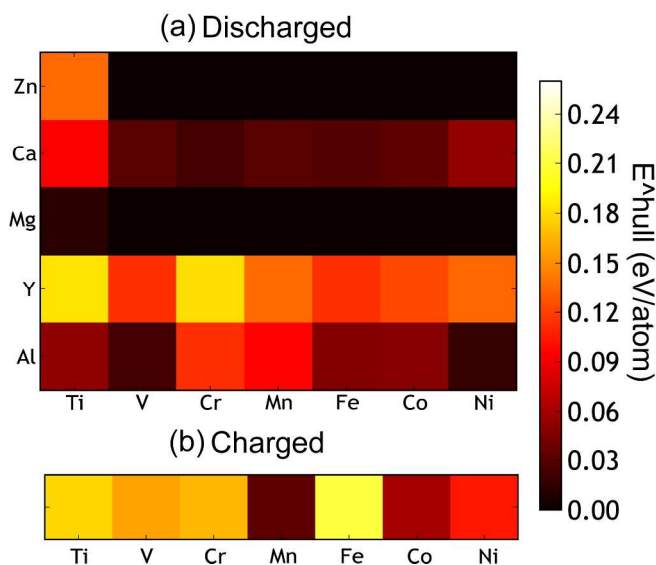


Fig. 5 a) The calculated thermodynamic stability of the AB_2O_4 spinel compounds as a function of the intercalating ion (vertical axis) and redox metal (horizontal axis).

(b) The energy above hull of the charged state which is calculated as the formation energy difference between a compound and the convex hull (see electronic supplemental information (ESI) for a detailed explanation).

The thermodynamic stabilities of the charged and discharged state are important considerations for possible cathode materials, as they may influence the cycle life as well as the synthesizability of the compounds. Thermodynamic stability can be measured by the driving force for a compound to separate into its most stable combination of compounds. From first principles, this is determined by comparing the energy of the compound with the convex energy hull of all ground states in the relevant phase diagram (see the electronic supplemental information (ESI) for a detailed explanation). Figure 5 (a) and (b) provide this energy above the hull of each compound. The ground state hulls were determined from all the calculated

compounds in the Materials Project database³⁶. A smaller energy above the hull implies that the material has a greater chance of being stable⁶³, e.g. at synthesis and upon cycling.

The Mg and Zn spinel phases (except ZnTi_2O_4) are all quite stable, exhibiting an energy above hull less than 0.011 eV/atom. Such a small value of the decomposition energy falls well within the accuracy of our calculations⁶³ or within relative changes between competing phases due to finite temperature effects. The Ca spinel structures are more thermodynamically unstable compared to the equivalent Mg and Zn compounds. This is consistent with Ca^{2+} normally preferring coordination environments larger than tetrahedral, though it is not excluded that this coordination can be achieved through electrochemical intercalation. The Y spinel compounds are the most unstable phases among all the candidates, due to the large ionic size of Y^{3+} . The Al^{3+} spinels are also relatively unstable in the discharged state. Among the chemistries of the charged host spinel, Mn_2O_4 forms the most stable structure. The high energy above hull for Fe_2O_4 suggests the difficulty to synthesize such a phase. Indeed, Fe^{4+} is only known to exist in ternary and higher component compounds⁶⁴ where the formation energy is lowered by the interaction with other cations. In terms of phase stability across both charged and discharged states, we conclude that MgMn_2O_4 , CaMn_2O_4 and ZnMn_2O_4 provide the best opportunities.

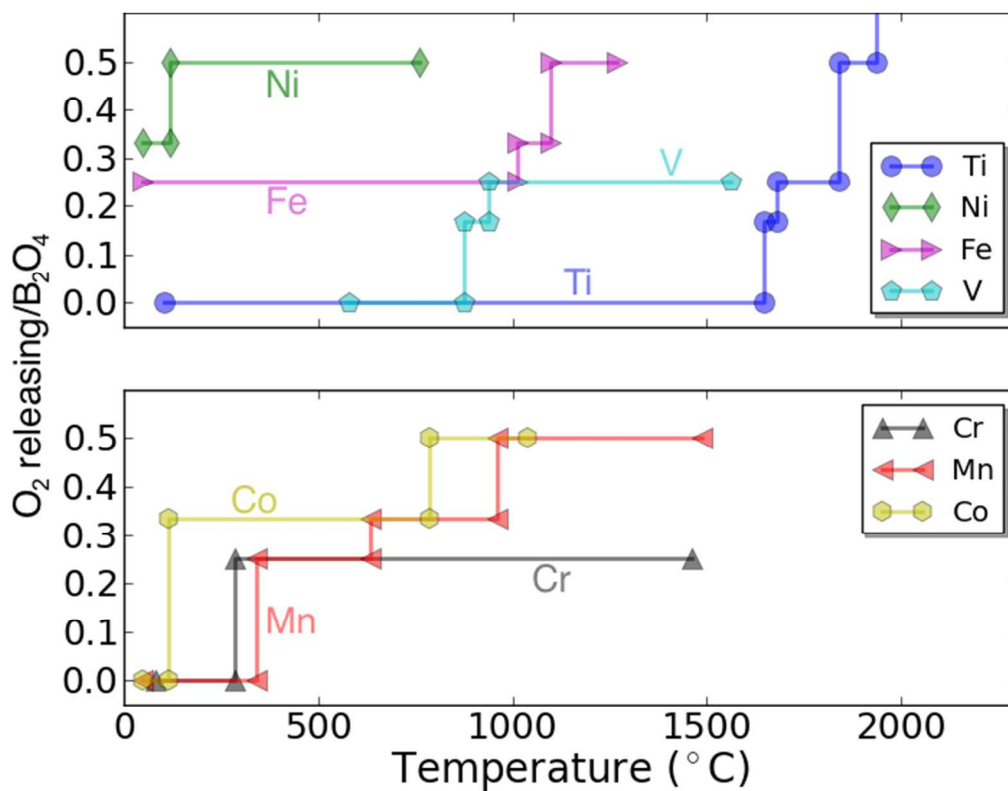


Fig 6. The calculated thermodynamic O₂ evolution diagram of charged host spinel compounds as a function of temperature. The vertical axis denotes how much O₂ is predicted to be released from the compound per formula unit of B₂O₄ as the material decomposes.

A way to gauge the intrinsic safety of a potential cathode material is by the thermal stability of the compound against O₂ release. The thermal stability can be estimated by calculating the temperature at which O₂ gas release is predicted thermodynamically (see Ref [43] and the ESI for more details on the methodology). Figure 6 shows the calculated O₂ amount released as a function of temperature for the charged spinel compounds (e.g. for B₂O₄), determined by the equilibrium

chemical potentials at which O₂ release can be expected. At low temperature the oxygen release is likely limited by kinetics and the decomposition temperatures should only be used to rank compounds relative to their oxidation strength. Clearly, the data in Figure 6 indicates that Fe₂O₄ and Ni₂O₄ are highly oxidizing, and are unlikely to be stable in their stoichiometric configuration at room temperature. Co₂O₄ decomposes to $\frac{2}{3}(\text{Co}_3\text{O}_4 + \text{O}_2)$ at a temperature slightly above 100 °C. The Cr₂O₄ and Mn₂O₄ spinels are predicted to decompose to Cr₂O₃ + $\frac{1}{2}\text{O}_2$ and Mn₂O₃ + $\frac{1}{2}\text{O}_2$ at 285 °C and 342 °C, respectively. Since the Mn spinel exists as a metastable phase in some Li batteries the Cr and Mn spinel phases should operate well at room temperature. Finally, the V₂O₄ and Ti₂O₄ spinels are predicted as fairly stable against O₂ release as indicated by their higher decomposition temperatures; 876 °C and 1646 °C, respectively. In summary, Ti₂O₄, V₂O₄, Cr₂O₄ and Mn₂O₄ are expected to exhibit superior thermal stability against O₂ release among the considered spinel compounds. Comparing the calculated voltage (Fig. 3) and thermodynamic stability (Fig. 5), a stable discharged phase and unstable charged phase naturally lead to higher voltage, and vice versa (as expected). For example, fairly unstable Fe₂O₄ and Ni₂O₄ result in a higher voltage, while Mn₂O₄ generally results in lower voltages.

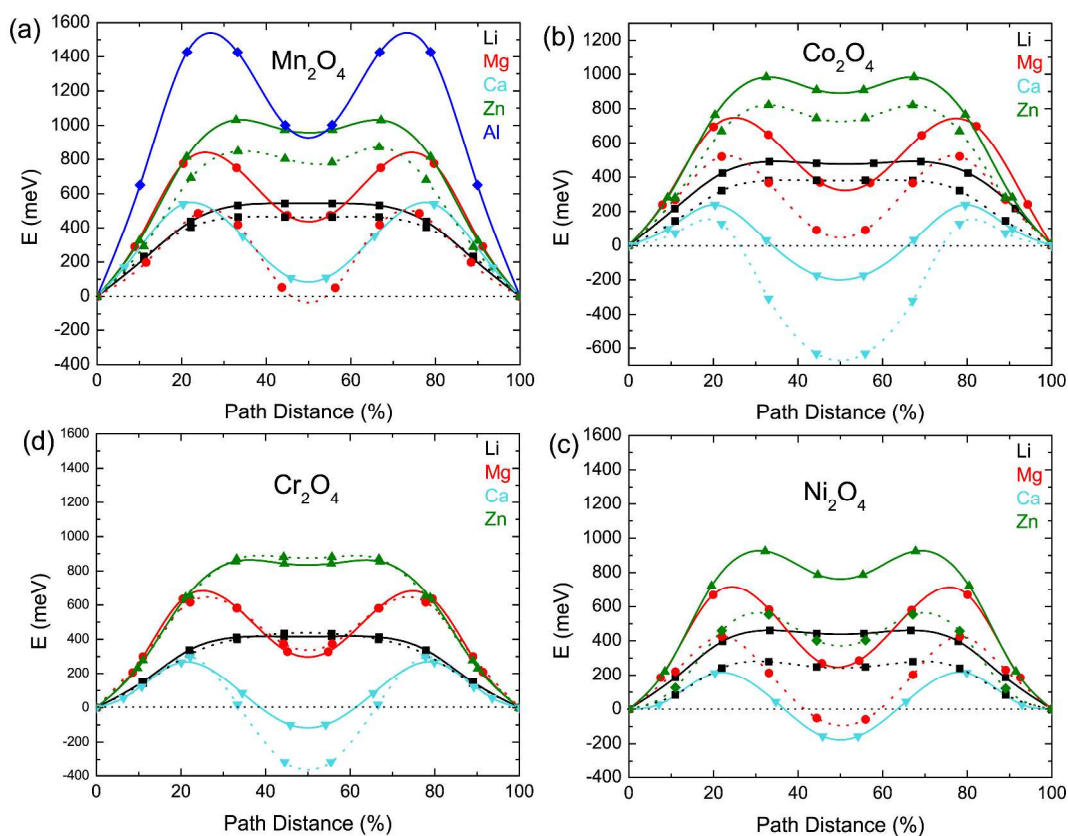


Fig. 7 Computed minimum energy paths for migration of different intercalants between the tetrahedral sites in the spinel B_2O_4 ($B = Mn, Co, Ni, Cr$) at the high vacancy limit (solid line) and dilute vacancy limit (dotted line), i.e. one mobile specie per supercell ($2 \times 2 \times 1$ of primitive cell).

The previous voltage, capacity and stability results for multivalent cathode materials show great potential to go beyond current Li-ion. However, a major remaining challenge is overcoming the sluggish diffusion expected for multivalent-ions. The slower diffusion of high-valent cations has been attributed to the stronger cation-anion interaction, which makes migrating $2+$ or $3+$ ions more difficult than moving $1+$ ions, though no quantitative information is available on multivalent ion

diffusion⁵. Hence, we calculate the migration energy barriers of the various multivalent ions ($A = \text{Mg}^{2+}$, Zn^{2+} , Ca^{2+} , Al^{3+} , and also Li^+ for comparison) in the spinel structure AB_2O_4 ($B = \text{Mn}$, Co , Ni , Cr) from first-principles as shown in Fig. 7. The Nudged Elastic Band method was used on both high vacancy limit and dilute vacancy limit corresponding a single migrating intercalant or a vacancy in an empty host or fully intercalated structure, showing the upper and lower limit of the intercalant migration activation barrier. To provide a general idea of how the migration energy barrier affects the diffusivity, a rough estimation can be given as follows: a migration barrier of ~ 525 meV corresponds to a typical ionic diffusivity of $\sim 10^{-12}$ cm²/s at room temperature, which approximately represents the lower limit for reasonable charge and discharge time (~ 2 hrs in micron-size active particles). Also, a 60 meV increase (decrease) in the migration energy corresponds to an order of magnitude decrease (increase) in the intercalant migration activation barrier. With smaller particle sizes a somewhat larger barrier can be tolerated: every order of magnitude in size reduction allows for two orders of magnitude smaller diffusion constant. Hence for 100nm particulates, migration barriers up to ≈ 645 meV may be acceptable.

In spinel Mn_2O_4 , which has been successfully commercialized for use in Li-ion batteries, Al^{3+} displays the highest diffusion barrier of ~ 1400 meV. Among the divalent cations, Zn^{2+} (~ 850 - 1000 meV) and Mg^{2+} (~ 600 - 800 meV) have the highest barriers, while Ca^{2+} is comparable to Li^+ (~ 400 - 600 meV). The migration barriers obtained for Li^+ in M_2O_4 ($M = \text{Mn}$, Co , Ni , Cr) all lie within ~ 400 to 600 meV in the

empty lattice limit, in good agreement with first-principles Li mobility calculations performed by Bhattacharya *et al.* in the spinel $\text{Li}_{1+x}\text{Ti}_2\text{O}_4$ system ($-1 < x < 1$)⁶⁵. Excluding the CrO_2 spinels and some of Ca-containing spinels, the migration barrier at high vacancy limit is always higher compared to the dilute vacancy limit, agreeing with Bhattacharya *et al.* that migration barrier is reduced by nearly 300 meV as Li is intercalated from the Li-deficient to the Li-rich limit (from ~ 600 meV for Li migration in Ti_2O_4 to ~ 300 meV for vacancy migration in LiTi_2O_4).⁶⁵ From kinetic Monte Carlo simulations, the room temperature self-diffusivity of Li was shown to span $\sim 10^{-10} - 10^{-9}$ cm²/s between $\text{Li}_{0.5}\text{Ti}_2\text{O}_4$ and LiTi_2O_4 , in good agreement with the excellent experimental rate-capability typically observed in Li spinel cathodes. Except in Mn_2O_4 , we could not converge the NEB for Al^{3+} due to the very large forces along the transition path, which is usually symptomatic of a very high barrier. The divalent barriers vary significantly with the chemical nature of the intercalant: Zn^{2+} ($\sim 800 - 1000$ meV), Mg^{2+} ($\sim 600 - 800$ meV), and Ca^{2+} ($\sim 200 - 500$ meV). Although Ca^{2+} migration appears to be facile in our calculations, only in Mn_2O_4 does Ca^{2+} prefer to occupy the tetrahedral site as opposed to the octahedral site (which can be observed in Fig. 7 as the energy along the migration path becomes negative when Ca is near the octahedral site in the Ni, Cr, and Co spinel). For this case, the migration barrier should be measured as the energy increase from the octahedral site to the maximum along the path (see Figure 7). We find that for all fully intercalated phases, the tetrahedral sites are more stable than the octahedral sites, which indicates a cross-over in site preference with concentration for some of the intercalating cations.

Discussion

Technical extrapolations of projected multi-valent (MV) chemistries to the cell level have shown that MV intercalation is one of the few technologies that can outperform Li-ion batteries in terms of energy density. In this paper we have used first principles calculations, well established in Li-cathode research^{2,3,43,63,66}, to evaluate the properties of MV-ion intercalation in spinel structures with different chemistries. We evaluated average insertion voltage, stability in the charged and discharged state, volume change upon intercalation, oxidation strength of the charged cathode, and the mobility of the multi-valent cations. Such first principles screening is important for this new field as multi-valent ion electrochemistry is not well established and, due to incompatibility between electrolytes and electrode materials, it can be difficult to obtain unambiguous experimental results on the performance of a specific cathode material^{4,67,68}. We found that the insertion voltage of Ca^{2+} , Mg^{2+} , Zn^{2+} , Al^{3+} and Y^{3+} against their respective metal anodes in general follows the electrochemical series but with quantitative variations due to the nature of the site preference of the intercalating ion. For example, Ca insertion voltages in spinels are lower than expected, as Ca in general prefers higher coordination than tetrahedral (commonly the most favorable site in the spinel structures). The Fe_2O_4 and Ni_2O_4 spinels are unlikely to function across the full capacity range due to the highly oxidizing and unstable nature of their fully charged states. As expected, Ti_2O_4 spinels have low insertion voltage for most intercalants, and in addition, are fairly unstable. The V_2O_4 and Cr_2O_4 spinels are also fairly unstable in the charged state,

and the V spinel exhibits a low insertion voltage for all intercalants besides Mg and Ca. From the perspective of stability, the most promising spinel chemistry is Mn_2O_4 as it is stable in the charged state and fairly stable in the discharged state for several intercalating ions. Intercalant mobilities are generally low due to the high activation energies when transitioning between the tetrahedral and octahedral site, though they are clearly not only controlled by charge. For example, among the divalent ions Zn mobility is inferior to Mg, and Ca may have fairly good mobility in the spinel. Al^{3+} intercalation into the spinel structure can likely be excluded from consideration even though it has the peculiar feature that volume changes upon insertion are very small. The activation barrier for motion is very high for Al^{3+} in Mn_2O_4 and its discharged spinels are all highly unstable. Somewhat surprisingly, and in contrast to experimental claims²⁹, we find that mobility of Zn in the spinel structure is very low, which in addition to its low insertion voltage, should exclude this system from further consideration for high energy density cathodes. The large intercalating ions such as Y^{3+} and Ca^{2+} are interesting, though the Y-spinels become unstable in the discharged limit. Both of these ions have reasonable insertion voltages and Ca^{2+} has better than expected migration barriers, due to its relative instability in the tetrahedral site. While this effect lowers the voltage from what would be expected by considering the electrochemical scale, it also seems to lower the migration barrier for motion. This may be similar to the more general principle that high energy defects in materials often have higher mobility.

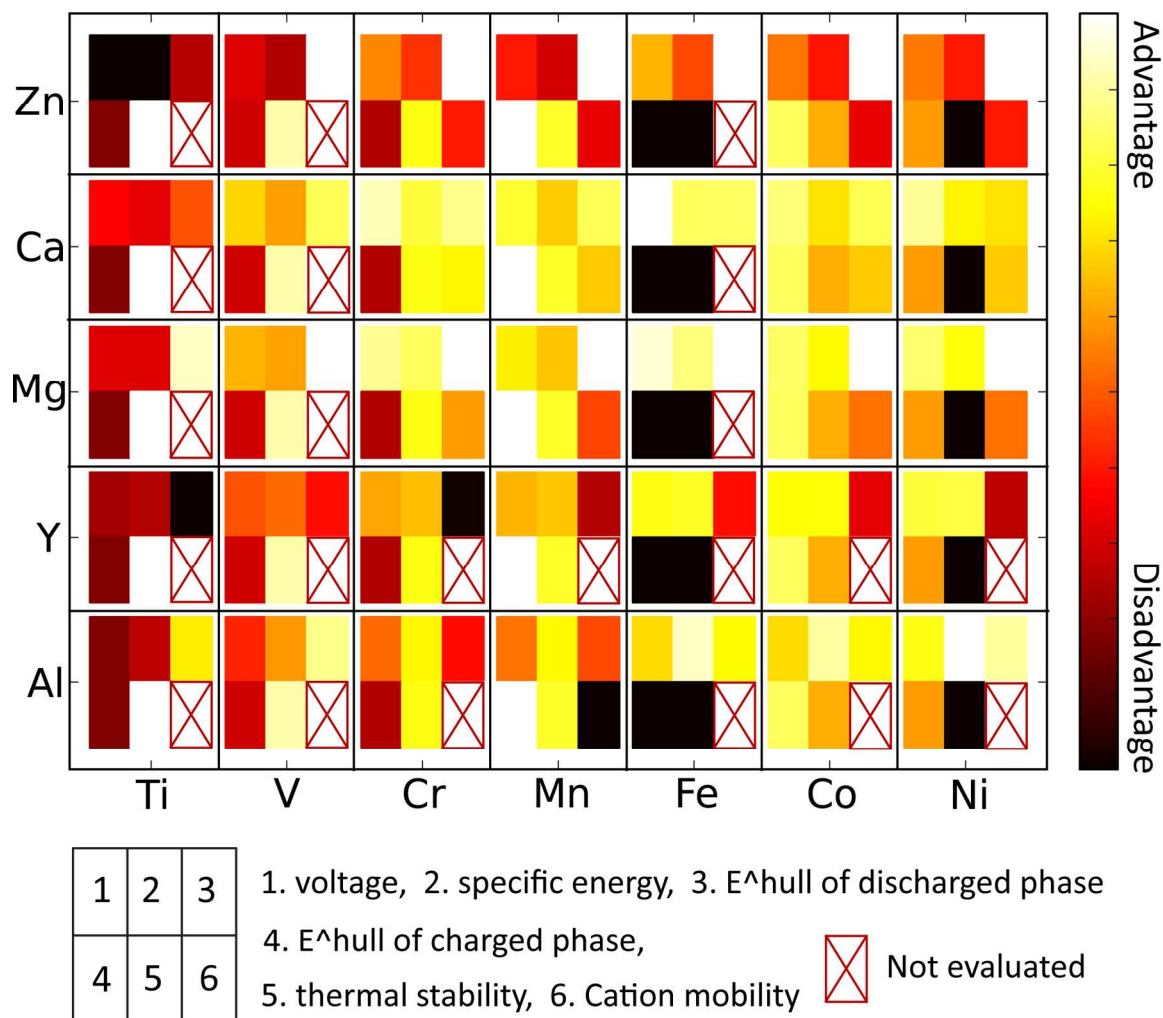


Fig. 8 Qualitative summary of multivalent spinel compounds based on multiple performance metrics, such as voltage, specific energy, thermodynamic stability of charged and discharged phases, thermal stability and intercalant mobility. The favorable (unfavorable) properties are represented with light (dark) color.

Considering all computed properties, Mn_2O_4 spinels are particularly interesting due to their stability. Among the divalent cations, both Mg^{2+} and Ca^{2+} may potentially be mobile in the spinel structure, warranting further experimental and computational

investigation (particularly at small particle sizes). Mixed spinel structures may provide a further promising avenue, as the $\text{Ni}^{4+/3+}$ and $\text{Co}^{4+/3+}$ show higher voltage than the $\text{Mn}^{4+/3+}$ redox couple and compounds such as LiNiMnO_4 are known to combine higher operating voltage with a relatively stable charged state^{24,25}. Improving the diffusivity should be a focus for all multivalent cathode materials.

Finally, a concern with spinels, as with all intercalation materials, is the occurrence of cation disorder. In the extreme case, normal spinels can convert to inverse spinels with part of the transition metals on the tetrahedral site. While in more common layered materials, lowering of the intercalant mobility by cation disorder is well understood through the contraction of the interlayer slab space by disorder⁶⁹, we are not aware of an equivalent study for spinels. Given the 3D and more rigid nature of the framework and the 3D diffusion network, one would expect spinels to be more tolerant to cation disorder. Nonetheless, we have performed a preliminary investigation into the driving force inverse spinel formation by adopting the same methodology as in Bhattacharya *et al.*⁵⁴. Based on small supercell calculations, we find that the normal spinel is always energetically favorable for Ca, Mg, Zn compounds (See Fig. S2 in the ESI). Further information can be obtained from the study of Burdett *et al.* who elucidated that cation disorder is strongly correlated to the relative size of the A and B ions.⁷⁰ Hence, Li and Zn prefer to form normal spinels, and we do not expect cation disorder. Ca is large and has the possibility to occupy octahedral sites that forms inverse spinel. Similarly, Mg may show cation site disorder for Ni, Fe, Co when synthesized at high temperature. However, in the case

that well ordered spinels cannot be formed at high temperature synthesis conditions, it may be still be possible to create the normal ordered spinel phase by chemical or electrochemical delithiation of the lithium spinels^{28,30} and inserting multi-valent cations.

In summary, we have performed systematic calculations to screen for and discover improved multivalent cathode materials using the spinel structure as a general host. On the basis of all property calculations, the spinel Mn_2O_4 is found to be a superior candidate with Ca^{2+} and possibly Mg^{2+} as mobile cations. It is our hope that our work provides a general guide and standard for future theoretical as well as experimental multivalent cathode development and design.

Acknowledgments

This work was intellectually led and fully supported by of the Joint Center for Energy Storage Research (JCESR), an Energy Innovation Hub funded by the U. S. Department of Energy, Office of Science, Basic Energy Sciences. Work at the Lawrence Berkeley National Laboratory was supported by the Assistant Secretary for Energy Efficiency and Renewable Energy, under Contract No. DEAC02-05CH11231. We also thank the National Energy Research Scientific Computing Center (NERSC) for providing computing resources. The Materials Project (BES DOE Grant No. EDCBEE) is acknowledged for infrastructure and algorithmic support.

References:

- (1) Goodenough, J. B.; Park, K.-S. The Li-Ion Rechargeable Battery: A Perspective. *J. Am. Chem. Soc.* **2013**, *135*, 1167–1176.
- (2) Hautier, G.; Jain, A.; Ong, S. P.; Kang, B.; Moore, C.; Doe, R.; Ceder, G. ChemInform Abstract: Phosphates as Lithium-Ion Battery Cathodes: An Evaluation Based on High-Throughput Ab Initio Calculations. *Chem. Mater.* **2011**, *42*, 3495.
- (3) Hautier, G.; Jain, A.; Mueller, T.; Moore, C.; Ong, S. P.; Ceder, G. Designing Multielectron Lithium-Ion Phosphate Cathodes by Mixing Transition Metals. *Chem. Mater.* **2013**, *25*, 2064–2074.
- (4) Yoo, H. D.; Shterenberg, I.; Gofer, Y.; Gershinshy, G.; Pour, N.; Aurbach, D. Mg Rechargeable Batteries: An on-Going Challenge. *Energy Environ. Sci.* **2013**, *6*, 2265.
- (5) Levi, E.; Levi, M. D.; Chasid, O.; Aurbach, D. A Review on the Problems of the Solid State Ions Diffusion in Cathodes for Rechargeable Mg Batteries. *J. Electroceramics* **2007**, *22*, 13–19.
- (6) Mitelman, a.; Levi, M. D.; Lancry, E.; Levi, E.; Aurbach, D. New Cathode Materials for Rechargeable Mg Batteries: Fast Mg Ion Transport and Reversible Copper Extrusion in $\text{Cu}_y\text{Mo}_6\text{S}_8$ Compounds. *Chem. Commun.* **2007**, 4212.
- (7) Persson, K.; Hinuma, Y.; Meng, Y. S.; Van der Ven, A.; Ceder, G. Thermodynamic and Kinetic Properties of the Li-Graphite System from First-Principles Calculations. *Phys. Rev. B* **2010**, *82*, 125416.
- (8) Lee, E.; Persson, K. a. Li Absorption and Intercalation in Single Layer Graphene and Few Layer Graphene by First Principles. *Nano Lett.* **2012**, *12*, 4624–4628.
- (9) Aurbach, D.; Lu, Z.; Schechter, a; Gofer, Y.; Gizbar, H.; Turgeman, R.; Cohen, Y.; Moshkovich, M.; Levi, E. Prototype Systems for Rechargeable Magnesium Batteries. *Nature* **2000**, *407*, 724–727.
- (10) Yu, W.; Wang, D.; Zhu, B.; Gui-en, Z. Intercalation of Mg in V_2O_5 . *Solid State Commun.* **1987**, *63*, 1043–1044.
- (11) Yu, W.; Zhu, B.; Wang, S.; Xus, L. Insertion of Bi-Valence Cations Mg^{2+} and Zn^{2+} into V_2O_5 . *Solid State Commun.* **1987**, *61*, 271–273.
- (12) Hayashi, M.; Arai, H.; Ohtsuka, H.; Sakurai, Y. Electrochemical Insertion/Extraction of Calcium Ions Using Crystalline Vanadium Oxide. *Electrochem. Solid-State Lett.* **2004**, *7*, A119.

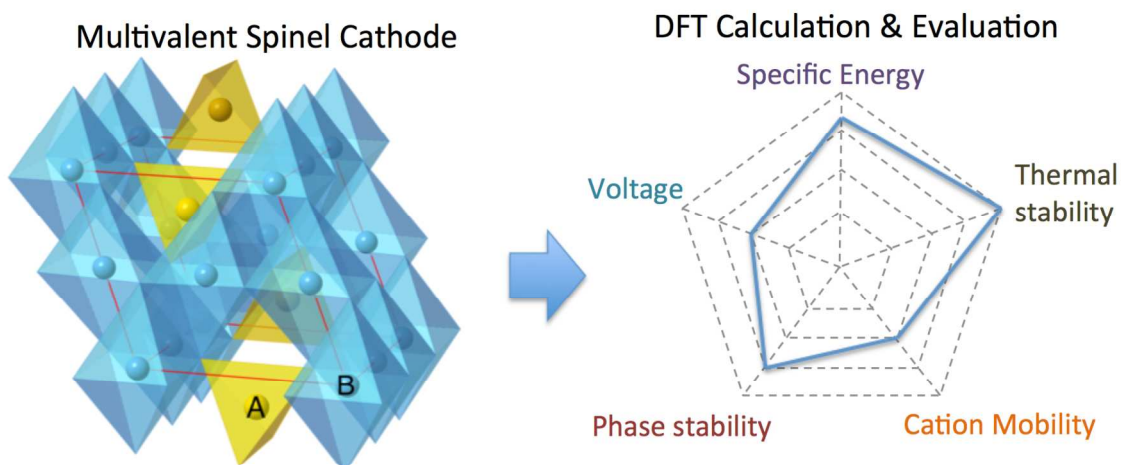
- (13) Spahr, M. E.; Novak, P.; Haas, O.; Nesper, R. Electrochemical Insertion of Lithium, Sodium, and Magnesium molybdenum(VI) Oxide. *J. Power Sources* **1995**, *54*, 346–351.
- (14) Sian, T.; Reddy, G. B. Infrared and Electrochemical Studies on Mg Intercalated α -MoO₃ Thin Films. *Solid State Ionics* **2004**, *167*, 399–405.
- (15) Gregory, T. D.; Hoffman, R. J.; Winterton, R. C. Nonaqueous Electrochemistry of Magnesium Applications to Energy Storage. *J. Electrochem. Soc.* **1990**, *137*, 775.
- (16) Amir, N.; Vestfrid, Y.; Chusid, O.; Gofer, Y.; Aurbach, D. Progress in Nonaqueous Magnesium Electrochemistry. *J. Power Sources* **2007**, *174*, 1234–1240.
- (17) Yuan, W.; Giinter, J. R. Insertion of Bivalent Cations into Monoclinic NbS₃ Prepared under High Pressure and Their Secondary Batteries. *Solid State Ionics* **1995**, *76*, 253–258.
- (18) Giraudet, J.; Claves, D.; Guérin, K.; Dubois, M.; Houdayer, A.; Masin, F.; Hamwi, A. Magnesium Batteries: Towards a First Use of Graphite Fluorides. *J. Power Sources* **2007**, *173*, 592–598.
- (19) Zheng, Y.; NuLi, Y.; Chen, Q.; Wang, Y.; Yang, J.; Wang, J. Magnesium Cobalt Silicate Materials for Reversible Magnesium Ion Storage. *Electrochim. Acta* **2012**, *66*, 75–81.
- (20) Le, D. B.; Passerini, S.; Coustier, F.; Guo, J.; Soderstrom, T.; Owens, B. B.; Smyrl, W. H. Intercalation of Polyvalent Cations into V₂O₅ Aerogels. *Chem. Mater.* **1998**, *4756*, 682–684.
- (21) Imhof, R.; Haas, O. Magnesium Insertion Electrodes for Rechargeable Nonaqueous Batteries – a Competitive Alternative to Lithium? *Electrochim. Acta* **1999**, *45*, 351.
- (22) Thackeray, M. M.; Bruce, P. G.; Goodenough, J. B.; Road, S. P. Lithium Insertion into Manganese Spinels. *Mat. Res. Bull.* **1983**, *18*, 461–472.
- (23) Thackeray, M. M.; Division, C. T.; Program, E. T. Manganese Oxides for Lithium Batteries. *Prog. Solid St. Chem.* **1997**, *25*, 1–71.
- (24) Amine, K.; Tukamoto, H.; Yasuda, H.; Fuiita, Y. A New Three-Volt Spinel Li₁ + Mn₁ . 5Ni₀ . 5O₄ for Secondary Lithium Batteries. *J. Electrochem. Soc.* **1996**, *143*, 1607–1613.

- (25) Terada, Y.; Yasaka, K.; Nishikawa, F.; Konishi, T.; Yoshio, M.; Nakai, I. In Situ XAFS Analysis of Li(Mn, M)₂O₄ (M=Cr, Co, Ni) 5V Cathode Materials for Lithium-Ion Secondary Batteries. *J. Solid State Chem.* **2001**, *156*, 286–291.
- (26) Kawai, H.; Nagata, M.; Kageyama, H.; Tukamoto, H.; West, A. R. 5 V Lithium Cathodes Based on Spinel Solid Solutions. *Electrochim. Acta* **1999**, *45*, 315–327.
- (27) Liu, D.; Lu, Y.; Goodenough, J. B. Rate Properties and Elevated-Temperature Performances of LiNi_{0.5-x}Cr_{2x}Mn_{1.5-x}O₄ (0 ≤ x ≤ 0.8) as 5 V Cathode Materials for Lithium-Ion Batteries. *J. Electrochem. Soc.* **2010**, *157*, A1269.
- (28) Sinha, N. N.; Munichandraiah, N. Electrochemical Conversion of LiMn₂O₄ to MgMn₂O₄ in Aqueous Electrolytes. *Electrochem. Solid-State Lett.* **2008**, *11*, F23.
- (29) Xu, C.; Du, H.; Li, B.; Kang, F.; Zeng, Y. Reversible Insertion Properties of Zinc Ion into Manganese Dioxide and Its Application for Energy Storage. *Electrochem. Solid-State Lett.* **2009**, *12*, A61.
- (30) Yuan, C.; Zhang, Y.; Pan, Y.; Liu, X.; Wang, G.; Cao, D. Investigation of the Intercalation of Polyvalent Cations (Mg²⁺, Zn²⁺) into λ -MnO₂ for Rechargeable Aqueous Battery. *Electrochim. Acta* **2014**, *116*, 404–412.
- (31) Zhou, F.; Cococcioni, M.; Marianetti, C.; Morgan, D.; Ceder, G. First-Principles Prediction of Redox Potentials in Transition-Metal Compounds with LDA+U. *Phys. Rev. B* **2004**, *70*, 235121.
- (32) Kresse, G.; Furthmüller, J. Efficient Iterative Schemes for Ab Initio Total-Energy Calculations Using a Plane-Wave Basis Set. *Phys. Rev. B. Condens. Matter* **1996**, *54*, 11169–11186.
- (33) Blochl, P. E. Projector Augmented-Wave Method. *Phys. Rev. B* **1994**, *50*.
- (34) Perdew, J. P.; Jackson, K. A.; Pederson, M. R.; Singh, D. J.; Foiles, C. M. Atoms, Molecules, Solids, and Surfaces: Applications of the Generalized Gradient Approximation for Exchange and Correlation. *Phys. Rev. B* **1992**, *46*.
- (35) Perdew, J.; Burke, K.; Ernzerhof, M. Generalized Gradient Approximation Made Simple. *Phys. Rev. Lett.* **1996**, *77*, 3865–3868.
- (36) Jain, A.; Ong, S. P.; Hautier, G.; Chen, W.; Richards, W. D.; Dacek, S.; Cholia, S.; Gunter, D.; Skinner, D.; Ceder, G.; *et al.* Commentary: The Materials Project: A Materials Genome Approach to Accelerating Materials Innovation. *APL Mater.* **2013**, *1*, 011002.

- (37) Ong, S. P.; Richards, W. D.; Jain, A.; Hautier, G.; Kocher, M.; Cholia, S.; Gunter, D.; Chevrier, V. L.; Persson, K. a.; Ceder, G. Python Materials Genomics (pymatgen): A Robust, Open-Source Python Library for Materials Analysis. *Comput. Mater. Sci.* **2013**, *68*, 314–319.
- (38) Wang, L.; Maxisch, T.; Ceder, G. Oxidation Energies of Transition Metal Oxides within the GGA+U Framework. *Phys. Rev. B* **2006**, *73*, 195107.
- (39) Aydinol, M. K.; Ceder, G. First-Principles Prediction of Insertion Potentials in Li-Mn Oxides for Secondary Li Batteries. *J. Electrochem. Soc.* **1997**, *144*, 1–4.
- (40) Aydinol, M.; Kohan, a.; Ceder, G.; Cho, K.; Joannopoulos, J. Ab Initio Study of Lithium Intercalation in Metal Oxides and Metal Dichalcogenides. *Phys. Rev. B* **1997**, *56*, 1354–1365.
- (41) Ong, S. P.; Wang, L.; Kang, B.; Ceder, G. Li - Fe - P - O 2 Phase Diagram from First Principles Calculations. *Chem. Mater.* **2008**, *77*, 1798–1807.
- (42) Jain, A.; Hautier, G.; Ong, S. P.; Moore, C. J.; Fischer, C. C.; Persson, K. a.; Ceder, G. Formation Enthalpies by Mixing GGA and GGA + U Calculations. *Phys. Rev. B* **2011**, *84*, 045115.
- (43) Ong, S. P.; Jain, A.; Hautier, G.; Kang, B.; Ceder, G. Thermal Stabilities of Delithiated Olivine MPO₄ (M=Fe, Mn) Cathodes Investigated Using First Principles Calculations. *Electrochem. commun.* **2010**, *12*, 427–430.
- (44) M. W. Chase. *NIST-JANAF Thermochemical Tables*; American Chemical Society: New York, 1998; p. 2013.
- (45) Wang, L.; Maxisch, T.; Ceder, G. A First-Principles Approach to Studying the Thermal Stability of Oxide Cathode Materials. **2007**, 543–552.
- (46) <http://pythonhosted.org/FireWorks>. *Http://pythonhosted.org/FireWorks*.
- (47) Henkelman, G.; Uberuaga, B. P.; Jonsson, H. A Climbing Image Nudged Elastic Band Method for Finding Saddle Points and Minimum Energy Paths. *J. Chem. Phys.* **2000**, *113*, 9901–9904.
- (48) Dathar, G. K. P.; Sheppard, D.; Stevenson, K. J.; Henkelman, G. Calculations of Li-Ion Diffusion in Olivine Phosphates. *Chem. Mater.* **2011**, *23*, 4032–4037.
- (49) Ong, S. P.; Chevrier, V. L.; Hautier, G.; Jain, A.; Moore, C.; Kim, S.; Ma, X.; Ceder, G. Voltage, Stability and Diffusion Barrier Differences between Sodium-Ion and Lithium-Ion Intercalation Materials. *Energy Environ. Sci.* **2011**, *4*, 3680.

- (50) Lin, H.; Wen, Y.; Zhang, C.; Zhang, L.; Huang, Y.; Shan, B.; Chen, R. A GGA+U Study of Lithium Diffusion in Vanadium Doped LiFePO₄. *Solid State Commun.* **2012**, *152*, 999–1003.
- (51) Xu, B.; Meng, S. Factors Affecting Li Mobility in Spinel LiMn₂O₄—A First-Principles Study by GGA and GGA+U Methods. *J. Power Sources* **2010**, *195*, 4971–4976.
- (52) Morgan, D.; Van der Ven, a.; Ceder, G. Li Conductivity in Li_xMPO₄ (M = Mn, Fe, Co, Ni) Olivine Materials. *Electrochem. Solid-State Lett.* **2004**, *7*, A30.
- (53) K. Amine, H. Tukamoto, H. Yasuda, Y. F. Preparation and Electrochemical Investigation of LiMn₂XO₄ (Me: Ni, Fe, and X = 0.5, 1) Cathode Materials for Secondary Lithium Batteries. *J. Power Sources* **1996**, *68*, 604–608.
- (54) Bhattacharya, J.; Wolverton, C. Relative Stability of Normal vs. Inverse Spinel for 3d Transition Metal Oxides as Lithium Intercalation Cathodes. *Phys. Chem. Chem. Phys.* **2013**, *15*, 6486–6498.
- (55) Gocke, E.; Schollhorn, R.; Aselmann, G.; Muller-Warmuthf, W. Molybdenum Cluster Chalcogenides Mo₆X₈: Intercalation of Lithium via Electron/Ion Transfer. *Inorg. Chem.* **1987**, *26*, 1805–1812.
- (56) McKinnon, W. R.; Dahn, J. R. Structure and Electrochemistry of Li_xMo₆S₈. *Phys. Rev. B* **1985**, *31*, 3084–3087.
- (57) Morita, M.; Yoshimoto, N.; Yakushiji, S.; Ishikawa, M. Rechargeable Magnesium Batteries Using a Novel Polymeric Solid Electrolyte. *Electrochem. Solid-State Lett.* **2001**, *4*, A177.
- (58) Wang, S.; Lu, Z.; Wang, D.; Li, C.; Chen, C.; Yin, Y. Porous Monodisperse V₂O₅ Microspheres as Cathode Materials for Lithium-Ion Batteries. *J. Mater. Chem.* **2011**, *21*, 6365.
- (59) Seng, K. H.; Liu, J.; Guo, Z. P.; Chen, Z. X.; Jia, D.; Liu, H. K. Free-Standing V₂O₅ Electrode for Flexible Lithium Ion Batteries. *Electrochem. commun.* **2011**, *13*, 383–386.
- (60) Ven, A. Van Der; Marianetti, C.; Morgan, D.; Ceder, G. Phase Transformations and Volume Changes in Spinel Li_xMn₂O₄. *Solid State Ionics* **2000**, *135*, 21–32.
- (61) Lee, J.; Urban, A.; Li, X.; Su, D.; Hautier, G.; Ceder, G. Unlocking the Potential of Cation-Disordered Oxides for Rechargeable Lithium Batteries. *Science* **2014**, *343*, 519–522.

- (62) Marianetti, C.; Morgan, D.; Ceder, G. First-Principles Investigation of the Cooperative Jahn-Teller Effect for Octahedrally Coordinated Transition-Metal Ions. *Phys. Rev. B* **2001**, *63*, 224304.
- (63) Hautier, G.; Ong, S. P.; Jain, A.; Moore, C. J.; Ceder, G. Accuracy of Density Functional Theory in Predicting Formation Energies of Ternary Oxides from Binary Oxides and Its Implication on Phase Stability. *Phys. Rev. B* **2012**, *85*, 155208.
- (64) Bergerhoff, G.; Brown, I. D. *Crystallographic Databases, F.H. Allen et Al. (Hrsg.) Chester, International Union of Crystallography*; 1987.
- (65) Bhattacharya, J.; Van der Ven, A. Phase Stability and Nondilute Li Diffusion in Spinel $\text{Li}_{1+x}\text{Ti}_2\text{O}_4$. *Phys. Rev. B* **2010**, *81*, 104304.
- (66) Jain, A.; Hautier, G.; Moore, C.; Kang, B.; Lee, J.; Chen, H.; Twu, N.; Ceder, G. A Computational Investigation of $\text{Li}_9\text{M}_3(\text{P}_2\text{O}_7)_3(\text{PO}_4)_2$ (M = V, Mo) as Cathodes for Li Ion Batteries. *J. Electrochem. Soc.* **2012**, *159*, A622.
- (67) Zhang, R.; Yu, X.; Nam, K.-W.; Ling, C.; Arthur, T. S.; Song, W.; Knapp, A. M.; Ehrlich, S. N.; Yang, X.-Q.; Matsui, M. A-MnO₂ as a Cathode Material for Rechargeable Mg Batteries. *Electrochem. commun.* **2012**, *23*, 110–113.
- (68) Song, W.; Arthur, T. S.; Bucur, C.; Matsui, M.; Muldoon, J.; Singh, N.; Zhang, R. HIGH VOLTAGE RECHARGEABLE MAGNESIUM CELL. *U.S. Pat.* **2013**, 0004830 A1.
- (69) Kang, K.; Ceder, G. Factors That Affect Li Mobility in Layered Lithium Transition Metal Oxides. *Phys. Rev. B* **2006**, *74*, 094105.
- (70) Burdett, J. K.; Price, G. D.; Pricelb, S. L. Role of the Crystal-Field Theory in Determining the Structures of Spinel. *J. Am. Chem. Soc.* **1982**, *104*, 92–95.



A matrix of spinel structures are systematically calculated and evaluated to screen for the improved multivalent battery cathode.